J. Fluid Mech. (1977), *vol.* 80, *part* 3, *pp.* 465–480
Printed in Great Britain

Stratified non-diffusive flow over a horizontal flat plate

By S. K. CHATURVEDI

Department of Mechanics, Mechanical and Aerospace Engineering, Illinois Institute of Technology, Chicago

AND G. S. JANOWITZ

Department of Geosciences, North Carolina State University, Raleigh

(Received 13 October 1976)

The effects of inertia on the upstream-growing boundary layer over a finite horizontal flat plate of length b moving uniformly with speed U_0 in a linearly stratified

$$[(d\rho/dy)_{-\infty} = -\rho_0\beta)],$$

viscous, non-diffusive fluid under the Boussinesq approximation are studied. The nonlinear inertia terms are linearized by the Oseen approximation, but no boundary-layer approximation is required. The flow is governed by two parameters, namely the internal Froude number $Fr\,[= U_0/(\beta g b^2)^{\frac{1}{2}}]$ and a parameter $L^3\,[= \beta g b^3/U_0\nu]$, where $L^{-\frac{3}{2}}$ is proportional to the ratio of boundary-layer thickness to plate length for the case $Fr = 0$. Large values of L^3 and $Fr^2 = 0$ correspond to the case of an upstream boundary layer. By increasing the Froude number gradually, a transition occurs from an upstream boundary layer accompanied by an upstream wake to a downstream boundary layer with a downstream wake. The upstream boundary layer and wake are characterized by a balance of viscous and buoyancy forces, whereas the downstream boundary layer and wake are characterized by a balance of inertia and viscous forces. In the so-called critical-boundary-layer case, $Fr^4L^3 = O(1)$, inertia, viscous and buoyancy forces are all important and this boundary layer is accompanied by both upstream and downstream wakes. Complete transition occurs when Fr^4L^3 increases from 10·0 to 1000·0. The drag on the plate is also calculated.

1. Introduction

The motion of a density-stratified fluid past obstacles is of great interest to meteorologists and oceanographers. Such flows possess features that are remarkably different from those produced in homogeneous fluids. To understand certain basic features of stratified flows, many investigators have considered the problem of a flat horizontal plate moving in an inviscid, linearly stratified, non-diffusive fluid. In the work of Yih (1959), the plate moves slowly enough that the nonlinear inertia terms can be completely neglected in the equations of motion. His solution describes upstream and downstream disturbances which do not decay owing to the absence of viscosity.

Martin & Long (1968) considered the same problem with viscosity. For slow motion of the flat plate, they discovered a similarity solution which describes a boundary layer whose thickness increases in the upstream direction from the trailing edge of the plate. This boundary layer is characterized by a balance of viscous and buoyancy forces and its thickness decreases towards the trailing edge of the plate as the one-fourth power of the distance from the trailing edge. This upstream-growing boundary layer stands in direct contrast to the more familiar downstream flat-plate boundary layer, which is characterized by a balance of inertia and viscous forces, in homogeneous flows. The phenomenon of the upstream boundary layer is characteristic of stratified flows and certain homogeneous rotating and magnetohydrodynamic flows. In the upstream boundary layer, the streamlines converge towards the trailing edge of the plate rather than diverging from the leading edge, as in the case in the Blasius boundary layer. Martin & Long also showed that the equation which describes the upstream boundary layer describes the upstream wake, but this equation, under the restrictive conditions of non-inertial, non-diffusive flow, cannot describe the downstream wake unless one of the above restrictions is relaxed. Martin (1966) gives an explanation for this based on a vorticity balance argument.

In their experimental investigation, Martin & Long confirmed the existence of an upstream-growing boundary layer under the above restrictions. Owing to limitations of their experimental set-up, they could not verify the similarity solution which describes the upstream wake. They also attempted to find the effect of inertia on the upstream boundary layer. They suspected that, as inertia increases, transition to a downstream-growing boundary layer must eventually occur. They towed the plate at the highest possible velocity permitted by their experimental set-up, but did not observe a downstream-growing boundary layer. Pao (1968) carried out a detailed experimental investigation and quantitatively confirmed the similarity solution describing the upstream wake.

During the course of our investigation Kelly & Redekopp (1972) studied stratified flow over a flat plate using similarity solutions. They determined that transition would occur when $Fr^4L^3 = O(1)$ in terms of the parameters used in this investigation although in this parameter regime their similarity techniques fail. The condition $Fr^4L^3 = O(1)$ is easy to understand. The ratio of vorticity generation by buoyancy to vorticity advection in the boundary layer, using the homogeneous boundary-layer thickness, is $1/Fr^4L^3$; using the Martin & Long boundary-layer thickness this ratio is $(Fr^4L^3)^{-\frac{1}{4}}$. Thus if $Fr^4L^3 = O(1)$, both advection and generation will be important. This will be verified here and the flow in this transitional regime will be computed.

In this investigation, we analyse the effect of inertia on the upstream boundary layer. Though the problem formulated here is similar to that considered by Kelly & Redekopp, our approach in solving it is entirely different. We use an integral approach similar to that adopted by Piercy & Winny (1933) and Miyagi (1964) for a homogeneous flow. This approach consists of finding the fundamental solution of Oseen's equation for stratified flow induced by a line momentum sink and then distributing these sinks along the plate such that the no-slip condition is satisfied on the plate. The solution of Oseen's equation for stratified fluid for a line momentum sink is due to Janowitz (1968). We shall use these results extensively in our investigation.

Quantitatively, our detailed results will not be as accurate as those obtained by boundary-layer techniques, where the latter apply, because we shall replace the non-linear inertia terms by an Oseen approximation. This model is strictly valid in the far field, and near the plate it may serve as a reasonable model for the inertia terms. From a qualitative viewpoint our model should be able to predict all the important aspects of the problem. It should be able to describe the upstream boundary layer, the homogeneous boundary layer, and the transition from one type to another. In addition, our model will give us a uniformly valid solution; a boundary-layer approximation will not be necessary. Thus we hope that our model will provide information about the entire flow field. In addition, it should be able to describe the transitional case in which inertia, buoyancy and viscous forces are equally important.

2. Formulation of the problem and the governing equation

A plate of length b is fixed in space (figure 1) and a fluid with a uniform speed U_0 and a linear density profile far upstream flows over it. The following are the non-dimensional equations which govern the steady two-dimensional flow of a viscous non-diffusive fluid under the Oseen model and Boussinesq approximation:

$$Fr^2\frac{\partial u}{\partial x}+\frac{\partial p}{\partial x}-\frac{1}{L^3}\left(\frac{\partial^2 u}{\partial x^2}+\frac{\partial^2 u}{\partial y^2}\right) = 0, \tag{1}$$

$$Fr^2\frac{\partial v}{\partial x}+\frac{\partial p}{\partial y}+\rho-\frac{1}{L^3}\left(\frac{\partial^2 v}{\partial x^2}+\frac{\partial^2 v}{\partial y^2}\right) = 0, \tag{2}$$

$$\partial u/\partial x+\partial v/\partial y = 0, \tag{3}$$

$$\partial \rho/\partial x - v = 0. \tag{4}$$

The boundary conditions become

$$u, v, p, \rho \to 0 \quad \text{as} \quad |x^2+y^2| \to \infty,$$

$$u(x,0) = -1, \quad v(x,0) = 0 \quad \text{for} \quad 0 \leqslant x \leqslant 1, \tag{5}$$

where $\qquad Re_b = U_0 b/\nu, \quad Fr^2 = U_0^2/\beta g b^2, \quad L^3 = Re_b/Fr^2 = \beta g b^3/U_0\nu,$

$$u = u'/U_0, \quad v = v'/U_0, \quad x = x'/b, \quad y = y'/b, \quad p = p'/\rho_0\beta g b^2, \quad \rho = \rho'/\rho_0\beta b.$$

Here, u', v', p' and ρ' represent the disturbances from the base flow quantities. The flow is governed by the two parameters Fr^2 and L^3. The parameter L^3 is the ratio of the buoyancy and viscous forces in this forced flow if $\partial/\partial x$, $\partial/\partial y = O(1)$.

In the governing equation the nonlinear inertia terms have been replaced by an Oseen-type linearization which is strictly valid in the far field, where the velocity perturbations become small. However, near the plate it should provide a reasonable model for inertial effects. Janowitz (1968) used the Oseen model to describe the flow in the far field due to a line singularity with finite drag force (a line momentum sink) moving with uniform velocity in linearly stratified, viscous fluid. His results are valid only in the far field but here they are used to describe the flow everywhere. The flow generated by the plate can be considered as being generated by a distribution of drag forces on the plate. From Janowitz's result we find that

$$u'(x', y', \xi') = D'(\xi')\, J(x'-\xi', y')/\mu,$$

where D' is the drag force per unit width, u' is the dimensional perturbation from a uniform velocity at (x', y'), $D'(\xi)$ is the dimensional drag force acting at $x'' = \xi'$, and J is a non-dimensional velocity perturbation given below. If we assume that the drag is continuously distributed over the entire plate, then we can write

$$du' = D''(\xi')\, d\xi' J(x'-\xi', y')/\mu,$$

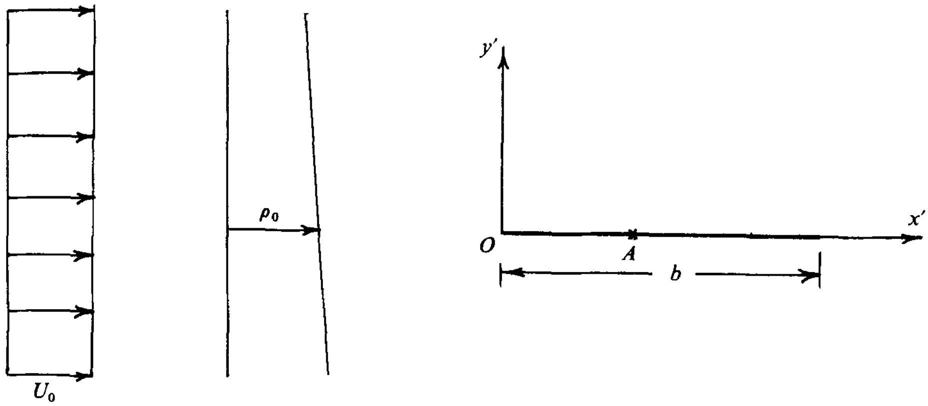

FIGURE 1. The geometry of the problem.

where $D''(\xi')$ is the drag per unit width per unit length of the plate. Integrating over the entire plate gives

$$u'(x',y') = \frac{1}{\mu}\int_0^b J(x'-\xi',y')\,D''(\xi')\,d\xi', \tag{6}$$

where J is known from Janowitz's solution. We seek to find a $D''(\xi')$ such that (5) is satisfied. Dividing by $U_0 b$, expression (6) becomes

$$u(x,y) = \int_0^1 D''(\xi)\,J(x-\xi,y)\,d\xi, \tag{7}$$

where

$$D(\xi) = D''(\xi)/(\mu U_0/b).$$

We next introduce a stream function ψ defined by

$$u = \partial\psi/\partial y, \quad v = -\partial\psi/\partial x,$$

and eliminate pressure and density from the governing equations to obtain the following vorticity equation:

$$\left(Fr^2\frac{\partial}{\partial x}-\frac{1}{L^3}\nabla^2\right)\nabla^2\psi+\frac{\partial\psi}{\partial x} = 0. \tag{8}$$

If we let $Fr^2 = 0$ and assume $\partial^2/\partial y^2 \gg \partial^2/\partial x^2$ we recover Martin & Long's equation:

$$\frac{1}{L^3}\frac{\partial^4\psi}{\partial y^4} = \frac{\partial\psi}{\partial x}. \tag{9}$$

In the limit $L^3 \to \infty$, we lose the highest-order derivative and accordingly we should expect that a boundary layer exists. This is indeed the case, as Martin & Long demonstrated. In the limit $Fr^2 \to \infty$ with Fr^2L^3 finite $(= Re_b)$ we recover the homogeneous Oseen equation.

3. Discussion of the solution for the line momentum singularity

A uniform flow with speed U_0 flows past a line singularity with finite drag/width D. The solution given by Janowitz is as follows.

For $x > 0$

$$J_+(x,y) = -\frac{1}{\pi}\int_0^{K_2^*} \frac{K^2 \exp(-\zeta_{1R}x)\sin(\zeta_{1I}x+\theta)\cos(Ky)\,dK}{\zeta_{1I}[(\zeta_{1R}-\zeta_3)^2+\zeta_{1I}^2]^{\frac{1}{2}}[(\zeta_{1R}-\zeta_4)^2+\zeta_{1I}^2]^{\frac{1}{2}}}$$
$$+\frac{1}{\pi}\int_{K_2^*}^{\infty}\left[\frac{K^2\exp(-\zeta_1 x)\cos(Ky)}{(\zeta_1-\zeta_2)(\zeta_1-\zeta_3)(\zeta_1-\zeta_4)}+\frac{K^2\exp(-\zeta_2 x)\cos(Ky)}{(\zeta_2-\zeta_1)(\zeta_2-\zeta_3)/(\zeta_2-\zeta_4)}\right]dK, \tag{10}$$

where
$$\theta = \tan^{-1}\left(\frac{\zeta_{1I}}{\zeta_{1R}-\zeta_3}\right)+\tan^{-1}\left(\frac{\zeta_{1I}}{\zeta_{1R}-\zeta_4}\right). \tag{11}$$

For $x < 0$
$$J_-(x,y) = -\frac{1}{\pi}\int_0^{\infty}\left[\frac{K^2\exp(-\zeta_3 x)\cos(Ky)}{(\zeta_3-\zeta_1)(\zeta_3-\zeta_2)(\zeta_3-\zeta_4)}+\frac{K^2\exp(-\zeta_4 x)\cos(Ky)}{(\zeta_4-\zeta_1)(\zeta_4-\zeta_2)(\zeta_4-\zeta_3)}\right]dK.$$

Here the ζ's are the roots of
$$(\zeta^2-K^2)^2+Re_\lambda\zeta^3+(1-Re_\lambda K^2)\zeta = 0. \tag{12}$$

For $K > K_2^*$ all the roots of (12) are real. $J(x,y)$ is the horizontal component of velocity at the point (x,y) due to a singularity at the origin and
$$\lambda = (U_0\nu/\beta g)^{\frac{1}{3}}, \quad Re_\lambda = U_0\lambda/\nu.$$

We note that, although there is no specified length scale in Janowitz's problem, λ occurs as the natural length scale; in the present case the plate length b is the characteristic length for non-dimensionalization. This gives us a slightly modified version of (12) for our case, i.e.
$$(\zeta^2-K^2)^2+L^3Fr^2\zeta^3+L^3(1-Fr^2K^2)\zeta = 0. \tag{13}$$

The horizontal velocity upstream and downstream of a point singularity located on the plate at $x=\xi$ is given by (10) and (11) with x replaced by $x-\xi$. Thus the term $J(x-\xi)$ in the integral representation is given by (10) or (11) depending on whether the point under consideration is downstream or upstream of the singularity. $J(x-\xi,y)$ satisfies the far-field boundary conditions, i.e. the perturbations die out, but we must also satisfy the no-slip condition on the plate, by requiring that $u(x,0) = -1$ in (7). We get the following integral equation for $D(\xi)$:
$$u(x,0) \equiv -1 = \int_0^1 J(x-\xi,0)D(\xi)\,d\xi, \quad 0 \leqslant x,\xi \leqslant 1. \tag{14}$$

We are faced with an integral equation whose kernel is extremely complex and is given in closed integral form by (10) or (11). Our aim is to determine the drag distribution function $D(\xi)$ such that (14), and hence the no-slip boundary condition, is satisfied.

4. Asymptotic theory for simplification of the kernel

In order to solve the integral equation analytically for $D(\xi)$, we simplify the kernel through assumptions based on the physical and mathematical nature of the problem. To begin with, we assume that the velocity at a point on the plate is primarily due to contributions from singularities in the immediate neighbourhood of that point. We also assume that the major contribution to the kernel $J(x-\xi, y)$ comes from large values of K. This follows from the mathematical nature of the problem. The reason for this is that the nature of the kernel $J(|x-\xi|, 0)$ for $|x-\xi| \to 0$ is revealed by the nature of its Fourier transform as $K \to \infty$. We first write, for $x-\xi < 0$,

$$J(x-\xi, 0) = -\frac{1}{\pi}\int_0^\infty f_{ex}(x-\xi, K)\, dK,$$

where

$$f_{ex} = K^2\left(\frac{\exp[-\zeta_3(x-\xi)]}{(\zeta_3-\zeta_1)(\zeta_3-\zeta_2)(\zeta_3-\zeta_4)} + \frac{\exp[-\zeta_4(x-\xi)]}{(\zeta_4-\zeta_1)(\zeta_4-\zeta_2)(\zeta_4-\zeta_3)}\right).$$

We rewrite the above expression as

$$\int_0^\infty (\ )\, dK = \int_0^{K_L} (\ )\, dK + \int_{K_L}^\infty (\ )\, dK,$$

where $K_L \gg 1$. We consider the asymptotic behaviour of the second integral only, because the first has a finite limit and behaves regularly. We also determine the roots of the quartic equation (12) for large values of K. Letting $K \to \infty$ in (8), we can show that the roots become

$$\zeta_1 = K - \frac{Fr^2L^3}{2} + \frac{Fr^4L^3}{8K} + \frac{1}{2Fr^2 K} + O(K^{-2}),$$

$$\zeta_2 = K - \frac{1}{2Fr^2K} + O(K^{-2}),$$

$$\zeta_3 = -\zeta_2, \quad \zeta_4 = -\zeta_1 - Fr^2L^3.$$

Substituting these expressions for ζ_1, ζ_2, etc., in the second integral and taking the limit $|x-\xi| \to 0$, we get the following expression for the second integral:

$$J_2(-|x-\xi|, 0) \approx -\frac{1}{4\pi}\int_{K_L}^\infty \left(\frac{1}{K} + |x-\xi|\right) \exp(-K|x-\xi|)\, dK.$$

Exactly the same expression is obtained for the downstream case. If we substitute $|x-\xi| = 0$ in the above expression we get

$$J_2(0,0) = -\frac{1}{4\pi}\int_{K_L}^\infty \frac{dK}{K} \to \infty.$$

We see that for large values of K and arbitrarily small non-zero values of $|x-\xi|$ the singularity is damped as we move away from it. The worst singularity ($\ln K$, $K \to \infty$) occurs at the point where the sink is located, but away from the sink it is damped owing to the factor $\exp(-K|x-\xi|)$ in both the upstream and the downstream case.

Next we replace $J_2(x-\xi, y)$ by

$$J_2(x-\xi, y) \approx -\frac{1}{4\pi}\int_0^\infty \left(\frac{1}{K+\delta} + |x-\xi|\right) \exp(-K|x-\xi|) \cos(Ky)\, dK. \qquad (15)$$

This step is essential because we want to invert the kernel analytically to get a closed-form expression for it. This can be done by either Fourier cosine or Laplace transform techniques, but the lower limit in (15) should be zero. δ is an undetermined constant which has been introduced to avoid introducing a singularity at $K = 0$. A method for determining δ has been described by Chaturvedi & Janowitz (1972). In effect we have assumed that the exact integrand is approximated well by its asymptotic expression for large K even for low values of K. This is justified in view of the fact that smaller K values do not contribute as significantly as do the large K values for $|x-\xi| \to 0$. Using the above idea we obtain.

$$J(|x-\xi|, y) = \frac{1}{4\pi}\operatorname{Re}\left\{\exp\left[\delta(|x-\xi|-iy)\right]\operatorname{Ei}(-\delta|x-\xi|-iy)+\frac{|x-\xi|^2}{y^2+|x-\xi^2|}\right\},$$

where

$$\operatorname{Ei}(-x) = -\int_x^\infty \frac{e^{-z}}{z}dz.$$

On the plate, $y = 0$ and

$$J(|x-\xi|, 0) = -\frac{1}{4\pi}(c-\ln|x-\xi|),$$

where $c = 0{\cdot}42-\ln\delta$. The integral equation becomes

$$4\pi = \int_0^1 [0{\cdot}42-\ln\delta-\ln(|x-\xi|)]\, D(\xi)\, d\xi.$$

Differentiating with respect to x we get

$$\int_0^1 \frac{D(\xi)}{|x-\xi|}d\xi = 0, \tag{16}$$

whose solution can be written as

$$D(\xi) = \bar{A}/[\xi(1-\xi)]^{\frac{1}{2}}, \quad \bar{A} = 4{\cdot}0/(0{\cdot}42-\ln\delta+2\ln 2).$$

Once the drag distribution has been determined, we can easily evaluate the horizontal velocity from

$$u(x,y) = \int_0^1 \frac{\bar{A}J(x-\xi, y)}{[\xi(1-\xi)]^{\frac{1}{2}}}d\xi,$$

where $J(x-\xi, y)$ is the exact expression. By integration this gives the perturbation stream function.

5. The no-slip condition on the plate

Since we have obtained the drag distribution function by using an approximate kernel, we expect that the no-slip condition on the plate will not be satisfied, i.e. $u(x,0) \not\equiv -1$, where

$$u(x,0) = \int_0^1 \frac{J(x-\xi)\,\bar{A}d\xi}{[\xi(1-\xi)]^{\frac{1}{2}}}, \quad 0 \leqslant x \leqslant 1.$$

The above expression involves a double integral which we evaluate in the following manner. Let A be any point on the plate where we wish to evaluate the velocity. Point A lies downstream of all singularities from 0 to A and is located upstream of all singularities from A to 1·0. From the asymptotic theory we know that for very small

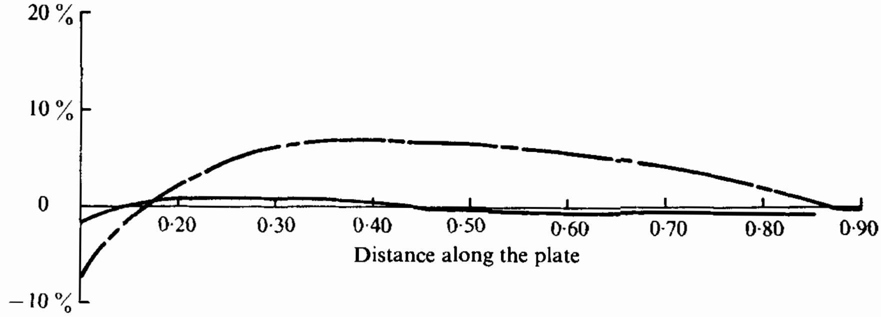

FIGURE 2. Error in the no-slip condition for $Fr^2 = 0$ and $L^3 = 10^5$. — — —, $D = 17{\cdot}2/[\xi(1-\xi)]^{\frac{1}{2}}$; ——, $D = 13{\cdot}4\ (1+1{\cdot}4\ \xi-1{\cdot}2\xi^2)/[\xi(1-\xi)]^{\frac{1}{2}}$.

values of $|x-\xi|$ we can approximate the exact kernel by the logarithmic kernel. Using that result we can divide the above integral into the following three parts:

$$u(x,0) = I_1+I_2+I_3,$$

$$I_1 = \int_0^{x-\epsilon} J_+(x-\xi,0)\,D(\xi)\,d\xi,$$

$$I_2 = \int_{x-\epsilon}^{x+\epsilon} (c+\ln\delta+\ln(|x-\xi|))\,D(\xi)\,d\xi,$$

$$I_3 = \int_{x+\epsilon}^{1\cdot0} J_-(x-\xi,0)\,D(\xi)\,d\xi.$$

In figure 2, the dashed line represents $u(x,0)+1$; it is clear that the no-slip condition is not satisfied exactly for this simple drag distribution function.

6. Evaluation of velocity profiles

We now compute the velocity profiles and streamlines for various interesting values of the parameters L^3 and Fr^2. The no-slip condition is checked for all cases before evaluating the flow field. In most cases the no-slip condition may be in error by as much as 10 %. For such cases the simple drag distribution is unsatisfactory, so that we use the following distribution function:

$$D(\xi) = \bar{A}[1+(\bar{B}/\bar{A})\,\xi+(\bar{C}/\bar{A})\,\xi^2]/[\xi(1-\xi)]^{\frac{1}{2}},$$

where $\bar{A}$, $\bar{B}$ and $\bar{C}$ are undetermined constants.

We note here that the dimensionless drag/unit width of the plate, $\bar{D}$, is given by

$$\bar{D} = \mu U_0 \int_0^1 D(\xi)\,d\xi,$$

or

$$\bar{D}/\mu U_0 = \pi\bar{A}[1+0{\cdot}5(\bar{B}/\bar{A})+0{\cdot}375(\bar{C}/\bar{A})]. \qquad (17)$$

Using the amended drag function reduces the error in the no-slip condition considerably (see figure 2). We may write

$$u(x,y) = \int_0^1 J(x-\xi,y)\,D(\xi)\,d\xi$$

$$= \bar{A}\int_0^1 \frac{J(x-\xi,y)\,[1+(\bar{B}/\bar{A})\,\xi+(\bar{C}/\bar{A})\,\xi^2]}{[\xi(1-\xi)]^{\frac{1}{2}}}\,d\xi,$$

or

$$u(x,y) = \bar{A}\left\{\int_0^1 \frac{J(x-\xi,y)}{[\xi(1-\xi)]^{\frac{1}{2}}}d\xi + \frac{\bar{B}}{\bar{A}}\int_0^1 \frac{\xi J(x-\xi,y)}{\xi(1-\xi)]^{\frac{1}{2}}}d\xi + \frac{\bar{C}}{\bar{A}}\int_0^1 \frac{\xi^2 J(x-\xi,y)\,d\xi}{[\xi(1-\xi)]^{\frac{1}{2}}}\right\}.$$

We evaluate the above three integrals and then choose suitable values of $\bar{A}$, $\bar{B}/\bar{A}$ and $\bar{C}/\bar{A}$ to minimize the error in the no-slip condition on the plate.

7. Discussion of results

We evaluate the flow field for $Fr^2 = 0$ and $L^3 = 10^5$, which corresponds to Martin & Long's case of the upstream boundary layer. The no-slip condition was in error by $\pm 8\,\%$ when we used the simple drag distribution function. Adding the linear and quadratic terms reduces the error to $\pm 2\,\%$ (see figure 2); in this case $\bar{A} = 13{\cdot}4$, $\bar{B}/\bar{A} = 1{\cdot}4$, $\bar{C}/\bar{A} = 1{\cdot}2$ and $\bar{D}/\mu U_0 = 52{\cdot}6$ while the solution of Martin & Long gives $\bar{D}/\mu U_0 = 3{\cdot}08 \times (L^3)^{\frac{1}{3}} = 3{\cdot}08 \times 10^{\frac{5}{3}} = 54{\cdot}8$. For large values of L^3, we expect the velocity profiles on the plate to be self-similar and to merge with the similarity solution of Martin & Long. From figure 3 it is quite evident that the velocity profiles computed from our model are in close agreement with the similarity profile. Closer agreement can be expected if we increase L^3 to still higher values.

Next, we compare velocity profiles in the upstream wake with Martin & Long's similarity profile, or the identical profile of Long (1959), and note (figure 4) that very good agreement exists. We also compare the streamline pattern of the flow field with that of Martin & Long. In the upstream wake closer agreement results as we move further upstream of the plate, but near the leading edge our solution differs greatly from that of Martin & Long since near the leading edge their solution blows up because of their boundary-layer approximation (figure 5). Over the plate, the streamlines computed from our model always converged towards the back of the plate as shown by Martin & Long (figure 6), and the streamline patterns are in good agreement. The horizontal velocity profiles show oscillations characteristic of stratified flows and the amount of overshoot predicted by our model is in good agreement with that predicted by Martin & Long. Thus we find that, qualitatively speaking, our model exhibits the same features as that of Martin & Long.

In the preceding case, the effects of inertia were absent. We wish to consider a case where inertial effects may be present but the flow is still subtransitional. According to Kelly & Redekopp transition will occur when $Fr^4L^3 = O(1)$; therefore we next consider the case $Fr^2 = 0{\cdot}001$ and $L^3 = 10^5$, which corresponds to $Re_b = 100$ and $Fr^4L^3 = 0{\cdot}10$. The no-slip condition is satisfied in the same fashion as before and in this case $\bar{A} = 10{\cdot}3$, $\bar{B}/\bar{A} = 2{\cdot}0$, $\bar{C}/\bar{A} = -1$, $\bar{D}/\mu U_0 = 52{\cdot}6$ while the maximum no-slip error is about $4\,\%$. The flow field exhibits the same features as in the preceding case and only the velocity profiles are given (figure 7); the overshoots are evident.

Next we compute the flow field for $L^3 = 10^5$ and $Fr^2 = 0{\cdot}003$, which corresponds to the case of a critical boundary layer in which inertia, buoyancy and viscous forces are all important ($Fr^4L^3 = 0{\cdot}9$). Here $\bar{A} = 13{\cdot}0$, $\bar{B}/\bar{A} = 1{\cdot}5$, $\bar{C}/\bar{A} = -1$, $\bar{D}/\mu U_0 = 56{\cdot}2$ and the maximum no-slip error is about $4\,\%$. In figure 8 we see that the velocity disturbance at $x = -1{\cdot}0$ is slightly less than in the preceding case with the overshoots still present and that a small but noticeable disturbance exists at $x = 1{\cdot}5$. This is in keeping with the fact that an upstream boundary layer with an upstream wake eventually has to switch

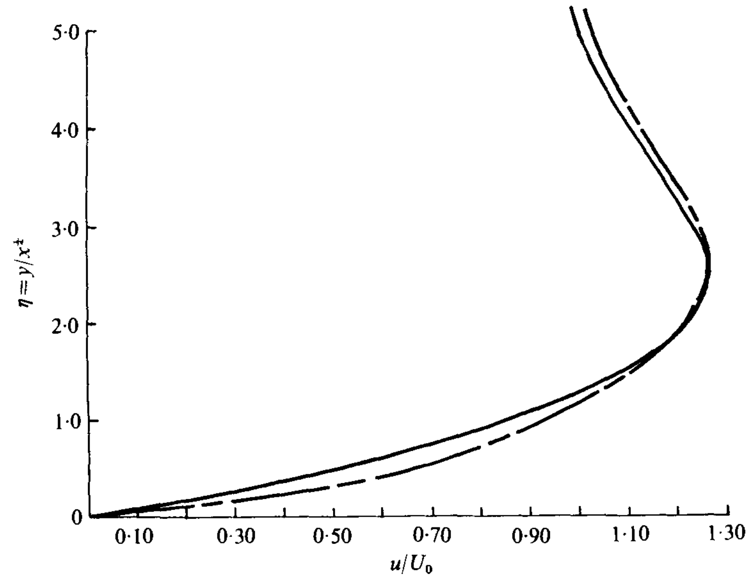

FIGURE 3. The horizontal velocity profile over the plate for $Fr^2 = 0$ and $L^3 = 10^5$. ——, Martin & Long's solution; — — —, present solution at $x = 0{\cdot}15$.

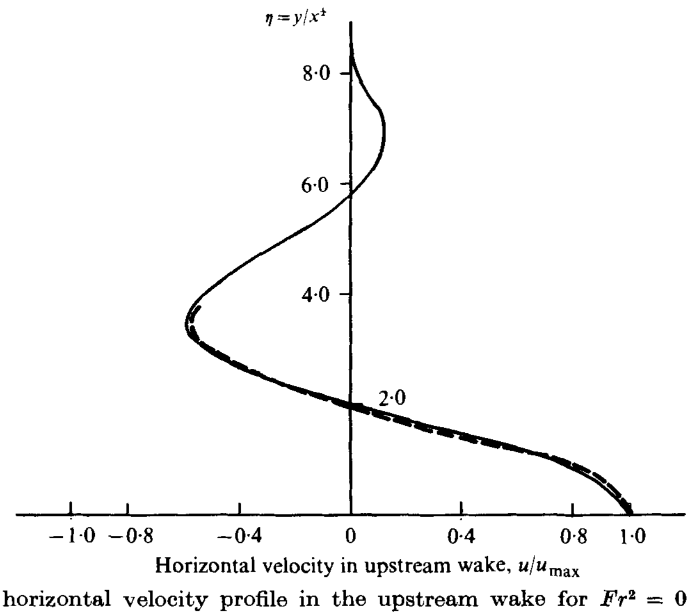

FIGURE 4. The horizontal velocity profile in the upstream wake for $Fr^2 = 0$ and $L^3 = 10^5$. ——, Martin & Long's solution; — — —, present solution at $x = -25{\cdot}0$.

to a downstream boundary layer accompanied by a downstream wake. The streamlines no longer converge towards the back of the plate; those near the plate, e.g. $\psi = 0{\cdot}01$ and $\psi = 0{\cdot}05$, diverge from the front of the plate and oscillate. Higher streamlines, i.e. $\psi = 0{\cdot}10$ and $0{\cdot}20$, still converge towards the back of the plate and they too oscillate (see figure 9). This suggests that for this case the flow field exhibits the characteristics of both types of boundary layer. For this case of a critical boundary

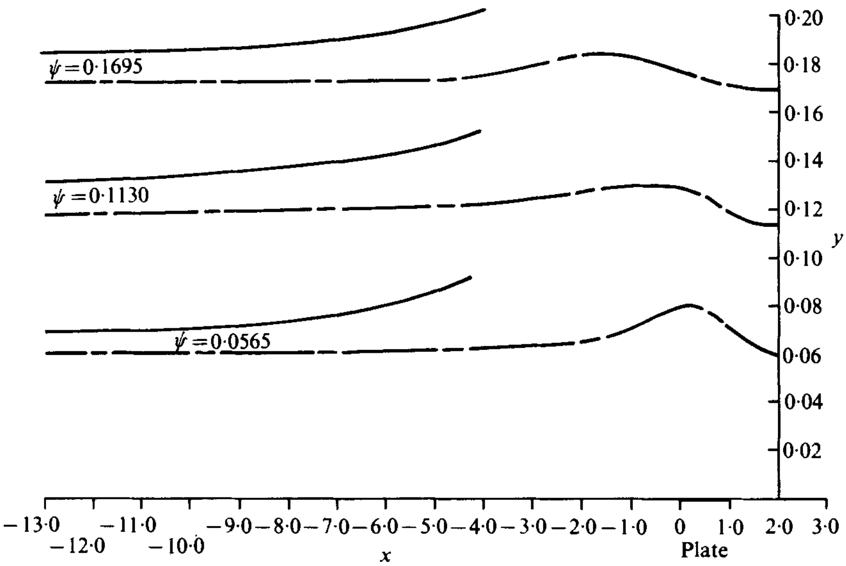

FIGURE 5. The streamline pattern of the flow field for $Fr^2 = 0$ and $L^3 = 10^5$. ——, Martin & Long's solution; — — —, present solution.

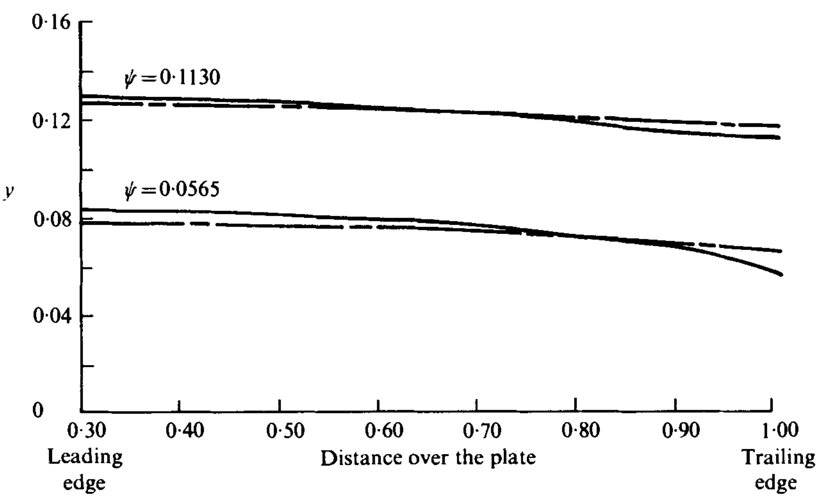

FIGURE 6. The streamline pattern over the plate for $Fr^2 = 0$ and $L^3 = 10^5$. ——, Martin & Long's solution; — — —, present solution.

layer no similarity solution can be found for which the outer flow is uniform. Our model does provide us with the qualitative features of the flow field for the case of a critical boundary layer. Transition is clearly starting to occur. Martin & Long attempted to observe transition by towing their plate at a speed of 1·9 cm/s with $b = 91{\cdot}5$ cm and $\beta g = 2{\cdot}62$, which corresponds to $Fr^3L^3 = 2{\cdot}2$. They did not observe a downstream-growing boundary layer, which is consistent with our calculations.

Next we increase Fr^2 to determine whether a complete transition to a downstream boundary layer has occurred. We choose the following values of the parameters: $L^3 = 10^5, Fr^2 = 0{\cdot}01\,(Fr^4L^3 = 10)$. Here $\bar{A} = 21{\cdot}8, \bar{B}/\bar{A} = 0{\cdot}45, \bar{C}/\bar{A} = -1, \bar{D}/\mu U_0 = 58{\cdot}2$

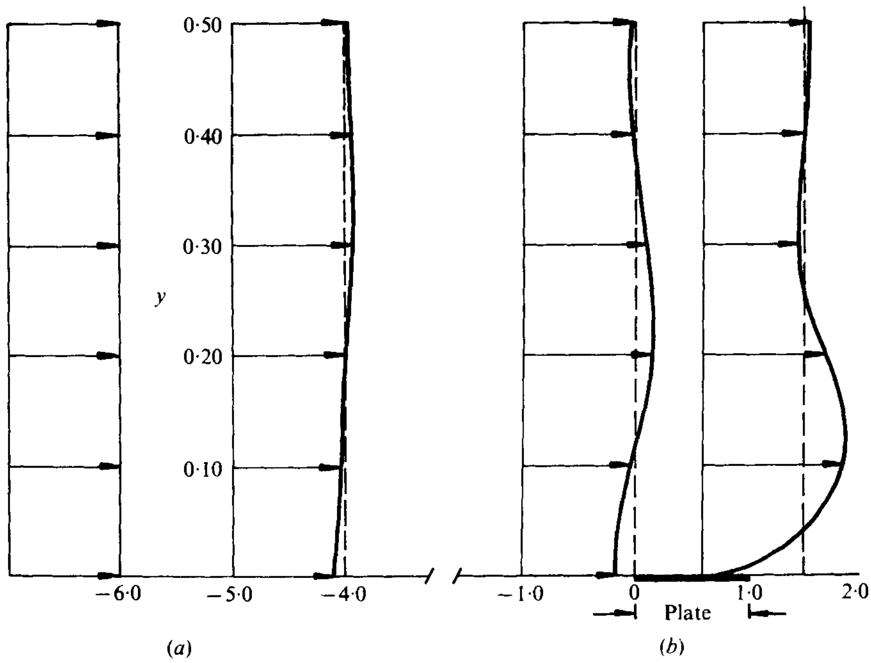

FIGURE 7. Horizontal velocity profiles upstream of and over the plate for $Fr^2 = 0{\cdot}001$ and $L^3 = 10^5$. (a) $x = -\infty$, (b) $x = 0{\cdot}6$.

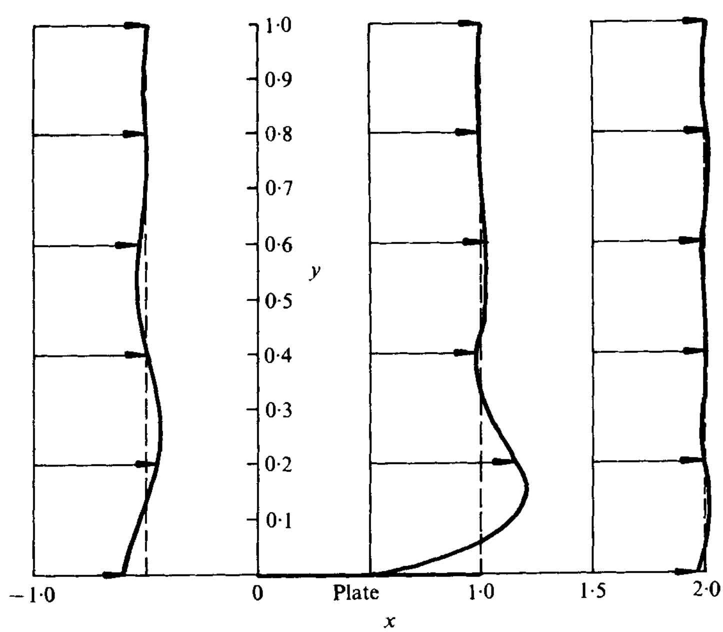

FIGURE 8. Horizontal velocity profiles for $Fr^2 = 0{\cdot}003$ and $L^3 = 10^5$.

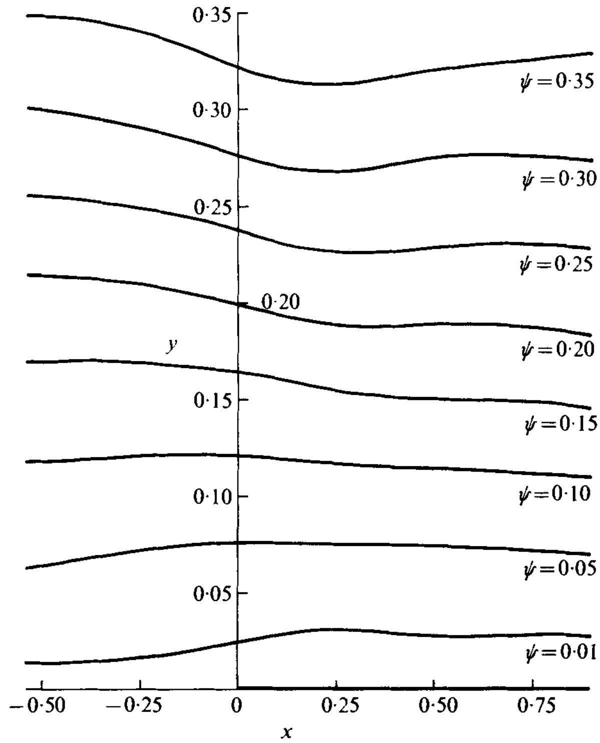

FIGURE 9. The streamline patterns over and upstream of the plate for $Fr^2 = 0{\cdot}003$ and $L^3 = 10^6$.

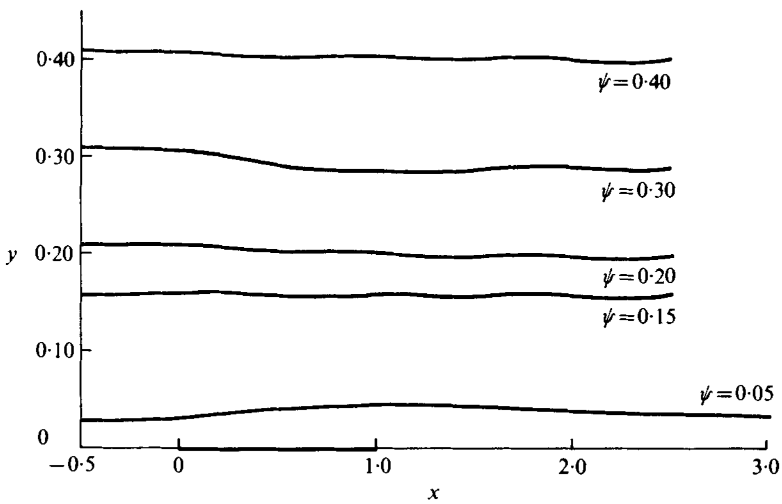

FIGURE 10. The streamline pattern for $Fr^2 = 0{\cdot}01$ and $L^3 = 10^5$.

and the no-slip error is at most 6 %. A streamline picture of the flow field suggests that a complete transition has not occurred. Streamlines close to the plate diverge from the front of the plate as in the case of a homogeneous boundary layer (see figure 10). Streamlines oscillate and the waviness can be interpreted as standing waves; this indicates that the buoyancy forces are still important.

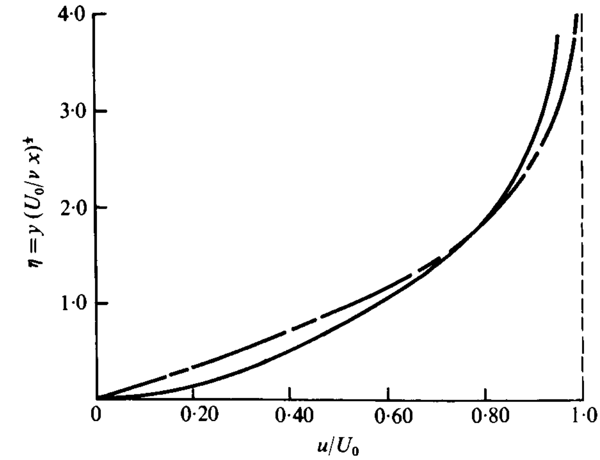

FIGURE 11. The horizontal velocity profile over the plate for $Fr^2 = 0{\cdot}10$ and $L^3 = 10^5$. — — —, Oseen solution; ——, present solution at $x = 0{\cdot}90$.

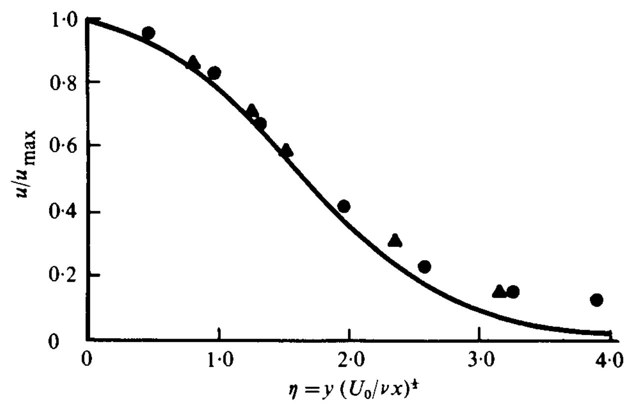

FIGURE 12. The horizontal velocity profile for $Fr^2 = 0{\cdot}10$ and $L^3 = 10^5$. ——, Goldstein's solution; ▲, present solution at $x = 41$; ○, present solution at $x = 61$.

Next we consider $L^3 = 10^5$ and $Fr^2 = 0{\cdot}10$, which corresponds to $Re_b = 10^4\,(Fr^4L^3 = 10^3)$. Here $\bar{A} = 100$, $\bar{B}/\bar{A} = -1{\cdot}0$, $\bar{C}/\bar{A} = 0{\cdot}4$, $\bar{D}/\mu U_0 = 204{\cdot}2$ and the maximum no-slip error is 3 %. Piercy & Winny give $\bar{D}/\mu U_0 = 2{\cdot}257 \times Re_b^{\frac{1}{2}} = 225{\cdot}7$ for homogeneous Oseen flow. This is the case of very high inertia and the upstream wake has completely disappeared, indicating that we are approaching the homogeneous limit. On the plate, the velocity profiles compare quite well with the profiles for the case of Oseen flow of a homogeneous fluid (figure 11) and the disturbance now extends far downstream. Very far downstream we expect the velocity profiles to be in close agreement with the similarity profile obtained by Goldstein (1930). A comparison of the velocity profile 60 plate lengths downstream with Goldstein's similarity profile shows excellent agreement (figure 12). We have also plotted some streamlines which lie very close to the plate (inside the boundary layer). From figure 13 we find that all streamlines now diverge from the leading edge of the plate and in the downstream wake they are brought back to their undisturbed heights. The waviness of the streamlines is absent, which suggests that generation of vorticity due to buoyancy in the upstream wake is absent. Another

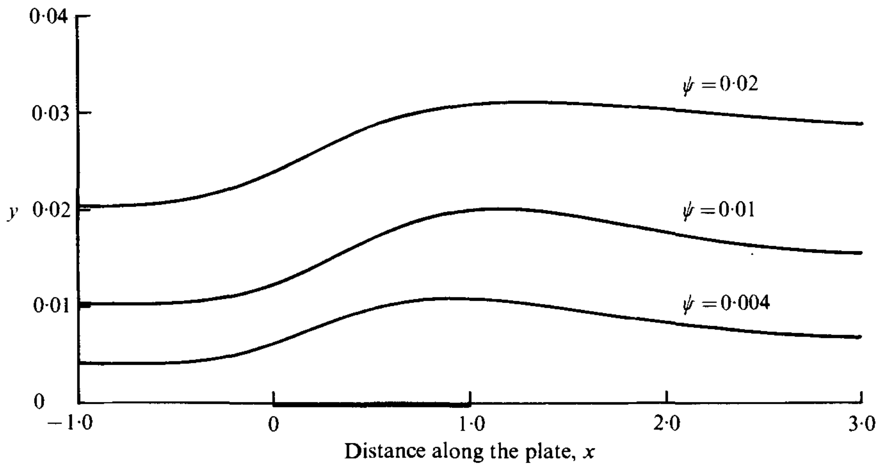

FIGURE 13. The streamline pattern for $Fr^2 = 0{\cdot}10$ and $L^3 = 10^5$.

important feature of stratified flows, the so-called jets or velocity overshoots, has almost disappeared. Thus we find that increasing the inertia forces switches the upstream boundary layer to a downstream layer.

8. Conclusions

The results show that our model qualitatively describes the features of the flow field for a wide range of the internal Froude number. During the course of this investigation Fr^2 was varied from 0 to 0·1 and Fr^4L^3 from 0 to 10^3. Large values of L^3 with $Fr^2 = 0$ correspond to the case of an upstream boundary layer. Martin & Long's boundary-layer approximation is valid only for large L^3 whereas our results are uniformly valid for all values of L^3, since no boundary-layer approximation was made in our analysis. A large value of L^3 and $Fr^2 = 0{\cdot}10$ corresponds to the case of a downstream-growing boundary layer and a downstream homogeneous wake. $Fr^2 = 0{\cdot}003$ and $L^3 = 10^5$ ($Fr^4L^3 = 0{\cdot}9$) corresponds to the case of a critical boundary layer which has the characteristics of both the boundary layers blended together, and no similarity solution to the equations for a critical boundary layer can be found for which the outer flow is uniform. Our model gives us a qualitative picture of the flow field for the case of a critical boundary layer. For this case and for the case $Fr^2 = 0{\cdot}01$ and $L^3 = 10^5$, we observe standing waves over the plate. We interpret the existence of these waves as a mechanism for dissipating the upstream wake. There is no sharp point of transition as the parameter Fr^2 varies. With increasing values of Fr^2, the upstream influence decreases whereas the downstream influence increases and eventually a complete switch takes place when $10 < Fr^4L^3 < 1000$. We also found that the drag coefficient predicted by our model is in close agreement with other existing results (e.g. Martin & Long 1968; Piercy & Winny 1933). For still higher values of Fr^2 we expect all important features of the stratified flow to disappear completely and in the limit we get the homogeneous case. Our modelling of the situation by Oseen flow confirms the assertion of Stewartson (1968) that Oseen's equation should provide us with the gross features of the flow field.

The authors acknowledge the support of the National Science Foundation under grant GA 31889 during the period in which this work was carried out.

REFERENCES

CHATURVEDI, S. K. & JANOWITZ, G. S. 1972 Stratified flow over a flat plate. *Fluid, Thermal Aerospace Sci. Dept., Case Western Reserve Univ., Cleveland, Ohio Tech. Rep.* TR-72-74.

GOLDSTEIN, S. 1930 Concerning some solutions of the boundary layer equations in hydrodynamics. *Proc. Camb. Phil. Soc.* **26**, 1–30.

JANOWITZ, G. S. 1968 On wakes in stratified fluids. *J. Fluid Mech.* **33**, 417.

KELLY, R. E. & REDEKOPP, L. G. 1970 The development of horizontal boundary layers in stratified flow. Part 1. Non-diffusive flows. *J. Fluid Mech.* **42**, 497.

LONG, R. R. 1959 The motion of fluids with density stratification. *J. Geophys. Res.* **64**, 2151.

MARTIN, S. 1966 The slow motion of a finite flat plate through a viscous stratified fluid. *Dept. Mech., Johns Hopkins Univ. Tech. Rep.* ONR21.

MARTIN, S. & LONG, R. R. 1968 The slow motion of a finite flat plate in a viscous stratified fluid. *J. Fluid Mech.* **31**, 669.

MIYAGI, T. 1964 Oseen flow past a flat plate inclined to the uniform stream. *J. Phys. Soc. Japan* **19**, 6.

PAO, Y. H. 1968 Laminar flow of a stably stratified fluid past a plate. *J. Fluid Mech.* **34**, 795.

PIERCY, N. A. V. & WINNY, H. F. 1933 *Proc. Roy. Soc.* A**140**, SA3.

STEWARTSON, K. 1968 On inviscid flow of a rotating fluid past an axially symmetric body using Oseen's equation. *Quart. J. Mech. Appl. Math.* **21**, 353.

YIH, C. S. 1959 Effect of density variation of fluid flow. *J. Geophys. Res.* **64**, 2219.